Lab on a Chip

PAPER

View Article Online
View Journal | View Issue

Hepatic organoids for microfluidic drug screening†

Cite this: *Lab Chip*, 2014, **14**, 3290

Sam H. Au,[ab] M. Dean Chamberlain,[abcd] Shruthi Mahesh,[ab] Michael V. Sefton[abc] and Aaron R. Wheeler*[abd]

Received 4th May 2014,
Accepted 20th June 2014

DOI: 10.1039/c4lc00531g

www.rsc.org/loc

We introduce the *microfluidic organoids for drug screening* (MODS) platform, a digital microfluidic system that is capable of generating arrays of individually addressable, free-floating, three-dimensional hydrogel-based microtissues (or 'organoids'). Here, we focused on liver organoids, driven by the need for early-stage screening methods for hepatotoxicity that enable a "fail early, fail cheaply" strategy in drug discovery. We demonstrate that arrays of hepatic organoids can be formed from co-cultures of HepG2 and NIH-3T3 cells embedded in hydrogel matrices. The organoids exhibit fibroblast-dependent contractile behaviour, and their albumin secretion profiles and cytochrome P450 3A4 activities are better mimics of *in vivo* liver tissue than comparable two-dimensional cell culture systems. As proof of principle for screening, MODS was used to generate and analyze the effects of a dilution series of acetaminophen on apoptosis and necrosis. With further development, we propose that the MODS platform may be a cost-effective tool in a "fail early, fail cheaply" paradigm of drug development.

Introduction

The current drug development paradigm is unsustainable. Of investigational new drugs (INDs) that enter Phase II (PhII) and Phase III (PhIII) clinical trials, 66% and 30% fail to transition into the next stage of development respectively, representing a significant loss of capital investment and opportunity (*i.e.*, resources that could have been directed towards successful candidates, instead).[1] It is widely recognized that a solution to this problem is to identify and eliminate INDs that are unlikely to pass clinical trials early in the development process – *i.e.*, "fail early, fail cheaply".[2] To accomplish this, the US Food and Drug Administration has stressed the need for *in vitro* screening tools that are capable of predicting toxicity and efficacy,[3] which together account for roughly 96% of PhII and PhIII attrition.[1] In the current paradigm, eight key *in vitro* assays are routinely used in early drug development[4] and have been designed to be compatible with conventional two-dimensional (2D) multiwell plates and robotic platforms for high-throughput IND screening. But the high rates of PhII and PhIII attrition suggests that these assays are ineffective in predicting *in vivo* clinical responses. This problem is particularly relevant for liver activity, as drug-induced hepatotoxicity is the most common cause of withdrawal of drugs from the market.[5]

A widely used method for improving the predictiveness of *in vitro* assays is to grow cells in an environment that better emulates that of cells *in vivo*. For example, liver cells have been cultured in 3D self-assembled spheroid aggregates[6–8] or suspended within hydrogels,[9–11] which greatly improves the degree of liver-specific function and enzymatic activity.[8,9,11] Although these methods have great promise, one of the reasons they have not been implemented routinely in the pharmaceutical industry is that the formation and addressing of these *in vivo*-like tissue constructs requires significant manual manipulation and skill; they are for the most part not well-suited for automated screening.

The tedium of 3D liver microtissue model assays can be addressed using microfluidics. For example, microfluidic liver cell assays have been reported that rely on 3D cell aggregates,[12–14] polylactic acid scaffolds,[15] microfibers,[16] compartmentalized micronetworks,[17,18] and cell-laden hydrogels.[19] When compared with traditional 2D liver cell culture, these systems have significant advantages for increasing metabolic function,[12,18] reconstituting native liver cell organization[14] and studying interactions of liver cells with other cell types.[13,15,17,19] However, as noted by Toner and coworkers,[18]

[a] *Institute of Biomaterials and Biomedical Engineering, University of Toronto, 164 College St., Toronto, ON, M5S 3G9, Canada. E-mail: aaron.wheeler@utoronto.ca; Fax: +1 (416) 946 3865; Tel: +1 (416) 946 3864*
[b] *Donnelly Centre for Cellular and Biomolecular Research, 160 College St., Toronto, ON, M5S 3E1, Canada*
[c] *Department of Chemical Engineering and Applied Chemistry, 200 College St., Toronto, ON, M5S 3E5, Canada*
[d] *Department of Chemistry, University of Toronto, 80 St George St., Toronto, ON, M5S 3H60, Canada*

† Electronic supplementary information (ESI) available. See DOI: 10.1039/c4lc00531g

a "fundamental limitation" of such systems is their inability to address individual constructs or wells within a single device. Stated a different way, all of the microfluidic systems for 3D liver cell culture that we are aware of[12–19] are "single pot" techniques, in which all of the cells in a given device are exposed to the same conditions. This limits the applicability of these tools for screening activities (*e.g.*, the evaluation of multiple INDs at different concentrations).

With these limitations in mind, we introduce a new method called *microfluidic organoids for drug screening* (MODS). MODS allows for the generation and culture of three dimensional micro-scale "organoids" containing liver cells, followed by analysis in an individually addressable format, enabling the evaluation of multiple IND candidates or concentrations on an automated device. MODS relies on digital microfluidics (DMF), an electrodynamic method of micro-scale (nanoliter to milliliter volumes) fluid manipulation.[20,21] DMF has recently been applied to live cell applications including the culture and analysis of cell lines,[22–25] micro-organisms,[26] cells in hydrogels,[27,28] and primary cells.[29] Importantly, a recent report confirmed that DMF actuation under typical operating conditions causes no observable detrimental effects on mammalian cell gene expression and DNA integrity.[30]

In comparison to the microfluidic methods for analyzing 3D liver constructs reported previously,[12–19] MODS is unique in the ability to address each tissue construct individually, allowing for the evaluation of different conditions simultaneously. Moreover, MODS allows for the automation of time-consuming processes such as the generation of mixtures and the formation of serial dilution series, all on devices with no moving parts and valve-less fluid manipulation. Furthermore, inexpensive DMF devices have recently been formed from paper[31], which suggests that future manifestations of MODS and related techniques may be useful for efficient screening of lead drug candidates rapidly and with low cost.

Materials and methods

Unless specified otherwise, general-use and cell-culture reagents were purchased from Sigma-Aldrich (Oakville, ON). Parylene-C dimer was obtained from Specialty Coating Systems (Indianapolis, IN). Teflon-AF 1600 was from DuPont (Wilmington, DE), and A-174 silane was from GE Silicones (Albany, NY). SU-8 3035 and SU-8 developer were from Microchem Corp. (Newton, MA). Photomasks were printed with 20 000 dpi resolution by Pacific Arts and Design (Toronto, ON). All working solutions were supplemented with 0.06% (wt/v) Pluronic F88 (BASF Corp., Florham park, NJ, USA) to limit fouling.[30,32] Unless specified otherwise, all experiments were replicated three times or more.

Device fabrication and operation

Digital microfluidic devices were fabricated in the University of Toronto Nanofabrication Centre (TNFC). Glass substrates bearing patterned chromium electrodes (used as bottom plates of DMF devices) were formed by photolithography and etching as described previously.[33] After patterning, the substrates were primed for Parylene-C coating by immersing them in silane solution (isopropanol, DI water, and A-174, 50 : 50 : 1 v/v/v) for 15 min, allowing them to air-dry and then washing with isopropanol. After priming, substrates were coated with Parylene-C (6.9 μm) by evaporating 15 g of dimer in a vapor deposition instrument (Specialty Coating Systems). SU-8 retention barriers were formed by pre-heating the substrates on a hot-plate at 95 °C for 5 minutes before spin coating ~5 mL SU-8 3035 for 10 s at 500 rpm followed immediately by a second 30 s spin at 1000 rpm. SU-8 coated substrates were ramp heated (~3 °C min^{-1}) on a hot-plate from 65 °C to 95 °C for 20 min before ramp cooling (~3 °C min^{-1}) to 65 °C. Substrates were exposed through a negative photomask for 10 seconds and then ramp heated on a hot-plate from 65 °C to 95 °C for 5 min before ramp cooling to 65 °C. Substrates were developed for 10 min in SU-8 developer, washed with isopropanol, dried with nitrogen gas and baked at 170 °C for 10 min. Finally, a 235 nm layer of Teflon-AF was spin-coated (1% in Fluorinert FC-40, 2000 rpm, 60 s) and the substrates were post-baked on a hot-plate (160 °C, 10 min). Unpatterned top plates were formed by spin-coating indium tin oxide (ITO) coated glass substrates (Delta Technologies, Stillwater, MN) with Teflon-AF (235 nm, as above). Devices were assembled with a patterned bottom plate and an unpatterned top plate joined by spacers formed from Scotch® double-sided tape (3M Canada, London, ON) (~180 μm thick). Droplets were manipulated by applying 220 V_{pp}, 5 kHz sinusoidal potentials to bottom-plate electrodes relative to the top-plate electrode using the DropBot open-source automated high-voltage switching system.[34]

Fig. 1 depicts the device geometry. Briefly, the bottom-plate device design comprises 65 electrodes, including a 2 × 17 array of 2.2 × 2.2 mm electrodes, five "large" reservoirs (10.0 × 6.5 mm) and four "small" reservoirs (8.4 × 4.0 mm). Each large reservoir is connected to the array by two 2.2 × 2.2 mm electrodes, while each small reservoir is connected to the array by four 1.5 × 1.5 mm electrodes. The 1.5 × 1.5 mm electrodes serve as "organoid culture regions", each with an SU-8 retention barrier. Each retention barrier features either fifteen 200 × 100 × 70 μm rectangular SU-8 pillars or fourteen 50 × 200 × 70 μm oval SU-8 pillars separated by 50 μm inter-pillar gaps.

Cell handling and preparation

HepG2 cells and NIH-3T3 cells were maintained separately in feed media [50/50 DMEM/F12 with 8% fetal bovine serum (FBS), 2% calf serum (CS), 100 IU mL^{-1} penicillin and 100 μg mL^{-1} streptomycin] by passaging every 3–4 days. For use in forming organoids, the two cell types were trypsinized with 0.25% trypsin–EDTA for 5 minutes at 37 °C followed by resuspension in separate centrifuge tubes in feed media at 4.0×10^7 cell mL^{-1} concentrations. Collagen–cell suspensions

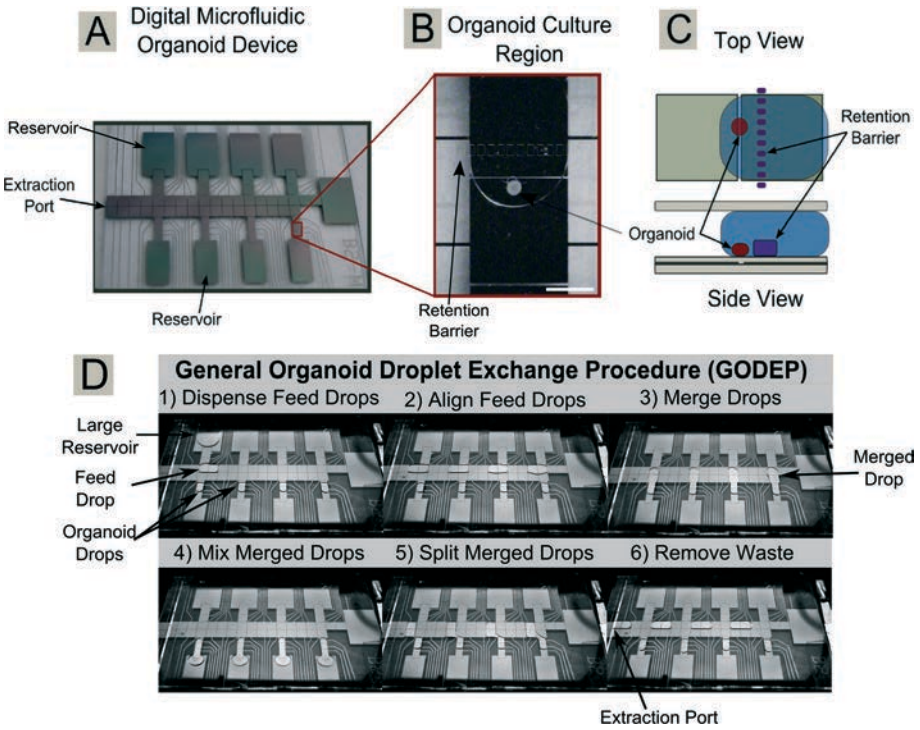

Fig. 1 Microfluidic organoids for drug screening (MODS). (A) Photograph of a MODS device. (B) Photomicrograph of the organoid culture region defined by a retention barrier (scale bar represents 0.75 mm). (C) Top-view (top) and side-view (bottom) schematics of MODS device. (D) General organoid droplet exchange procedure (GODEP) for reagent/dye exchange and sample extraction. See online ESI† for a detailed examination of droplet mixing efficiency.

were prepared on ice in 1.5 mL microcentrifuge tubes by combining and mixing the solutions listed in Table 1 from 3D collagen cell culture kits using pipette aspiration (Millipore, Inc., Billerica, MA).

Organoid formation and reagent exchange

Device top and bottom plates were washed separately with 70% ethanol and allowed to air dry in a laminar flow hood prior to assembly with spacers. 6.0 μL aliquots of collagen–cell suspensions were electrodynamically loaded onto small reservoirs and 315 nL droplets were dispensed onto 1.5 × 1.5 mm driving electrodes adjacent to SU-8 retention barriers. The droplets were allowed to gel (forming organoids) for 1 hour at 37 °C/5% CO_2. The organoids were then "fed" with feed media using a process that that we call the "general organoid droplet exchange procedure" (GODEP), which is depicted in Fig. 1D. GODEP delivers fresh media or reagents to organoids and removes spent media from devices for subsequent analysis. Briefly, in a typical GODEP, 12 μL aliquots of feed media (or other reagents, as described below) are loaded into 10.0 × 6.5 mm reservoirs and then 1.36 μL droplets are dispensed onto the 2.2 × 2.2 mm electrode array. Up to four of these droplets are independently delivered to organoid-containing droplets, and the merged contents are mixed by actuation across five linear electrodes in the organoid culture region (see the online ESI† for an analysis and discussion of mixing in GODEP). Media in excess of 630 nL (equivalent to the volume associated with two 1.5 × 1.5 mm electrodes) are then dispensed from merged droplets for extraction either to waste or for subsequent analysis from the edge of the device using a blunt tip 24 gauge needle connected to a 1 mL syringe.

Table 1 Liver organoid components. Volumes (μL) of components used to create collagen–cell suspensions which gel to become organoids

Component	Co-culture 0.9 mg mL^{-1} collagen	Mono-culture 0.9 mg mL^{-1} collagen	Co-culture 1.5 mg mL^{-1} collagen	Mono-culture 1.5 mg mL^{-1} collagen
Collagen I	80	80	80	80
5× DMEM	20	20	20	20
Feed media	166	181	61	70
10% (wt/v) F88	1.8	1.8	1.1	1.1
Neutralization buffer	2.5	2.5	2.5	2.5
4.0×10^7 HepG2 mL^{-1}	15	15	9.1	9.1
4.0×10^7 NIH-3T3 mL^{-1}	15	0	9.1	0

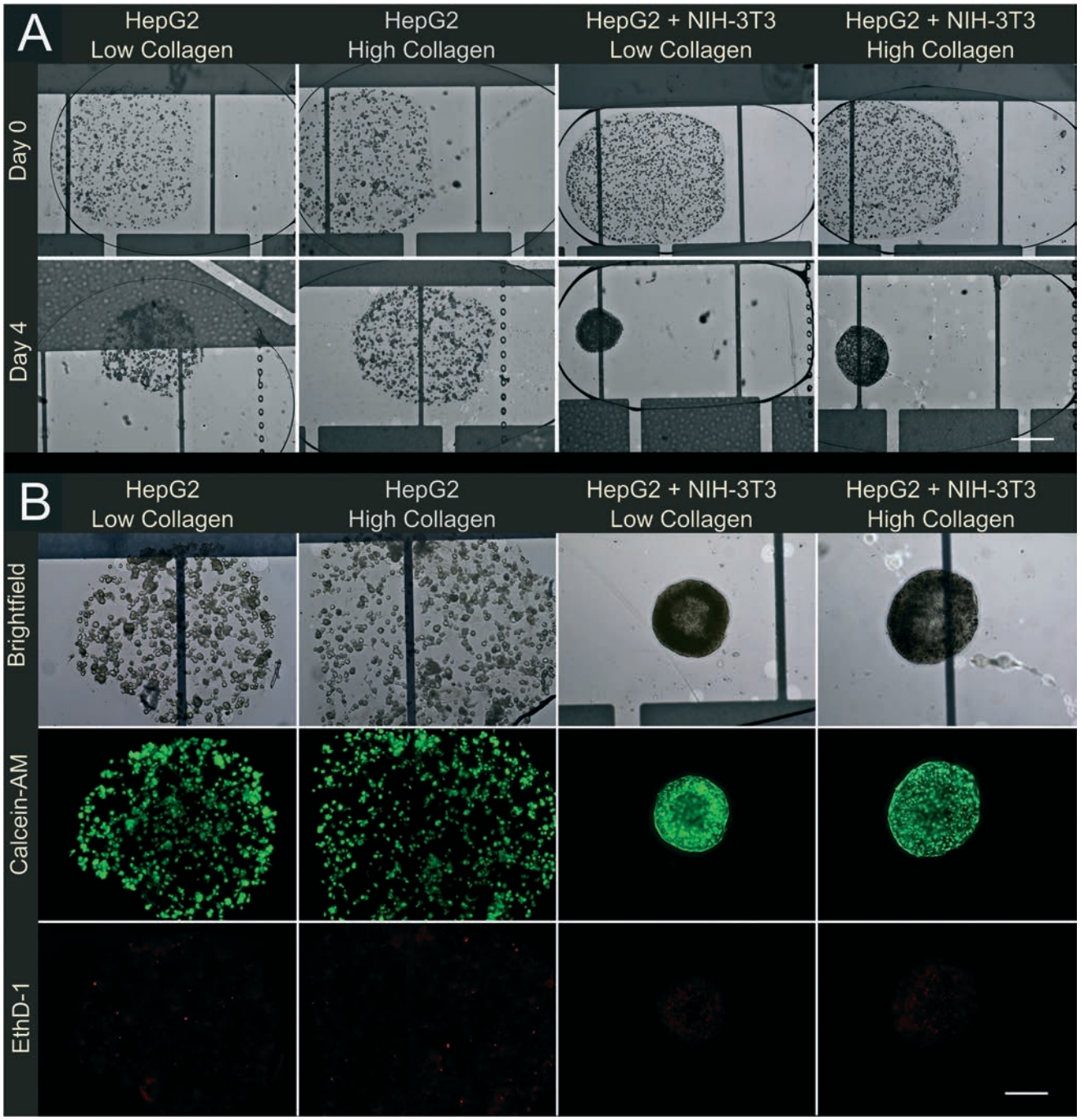

Fig. 2 Liver organoid contractility and viability. (A) Photomicrographs of representative organoids cultured on MODS platform on day 0 (top) and day 4 (bottom) after gel formation. Organoids were seeded with HepG2 cells (2×10^6 cell mL^{-1}) with or without NIH-3T3 fibroblasts (2×10^6 cell mL^{-1} each) in low (0.9 mg mL^{-1}) or high (1.5 mg mL^{-1}) density collagen. Scale bar represents 200 μm. (B) Photomicrographs of representative organoids cultured on a DMF platform 4 days after gel formation in brightfield (top), stained for viability with calcein-AM (green, middle) and stained for cell death with ethidium homodimer-1 (red, bottom). Organoids were seeded with HepG2 cells (2×10^6 cell mL^{-1}) with or without NIH-3T3 fibroblasts (2×10^6 cell mL^{-1} each) in low (0.9 mg mL^{-1}) or high (1.5 mg mL^{-1}) density collagen. Scale bar represents 100 μm.

Viability and contractility assays

Liver organoids were formed on device, incubated at 37 °C/5% CO_2 and maintained by feeding with feed media using GODEP (as described above) every day for four days. On the fourth day, PBS droplets containing 5.86 μM calcein AM and 11.72 μM ethidium homodimer-1 (Life Technologies, Inc., Burlington, ON, Canada) were merged with organoid droplets (to final concentrations of 4 μM and 8 μM respectively). Merged droplets were mixed and excess media split from organoid cultures. Organoids were incubated at room temperature for 30 minutes before washing with PBS droplets

using GODEP and analyzed using microscopy (Leica DM2000, Leica Microsystems Canada).

Albumin analysis

Liver organoids were formed and maintained as above except that droplets containing spent media were removed from devices during GODEP on days 1–4 and frozen in 0.6 mL microcentrifuge tubes at −80 °C until analysis. Albumin levels were quantified using a human albumin enzyme-linked immunosorbent assay (ELISA) Kit (Abnova Corporation, Taipei, Taiwan) following the manufacturer's recommended guidelines. The measured albumin levels were dilution-adjusted by multiplying the values by 3.16 [the ratio of the merged droplet volume (1.99 μL) to that of the culture organoids volume (0.63 μL)] to obtain the concentration of albumin in organoid culture droplets.

Enzymatic activity assay

Liver organoids were formed in the same manner as above as HepG2 & NIH-3T3 co-culture constructs. GODEP was used to introduce feed media containing reagents and remove an equal volume of excess liquid to organoid cultures daily. Three populations of organoids were treated for three consecutive days: control, induced, and induced-inhibited. Control organoids were fed on days one and two with 1.36 μL feed droplets containing 1.46% (v/v) ethanol (to a final concentration in the organoid droplet of 1.0 %). Induced and induced-inhibited organoids were fed on day one with 1.36 μL feed droplets containing 14.6 mM dexamethasone and 1.46% (v/v) ethanol (to concentrations in the organoid droplet of 10.0 mM and 1.0%, respectively) and on day two with feed droplets containing 10.0 mM dexamethasone and 1.0% ethanol. Control and induced organoids were fed on day three with 1.36 μL feed droplets containing 0.146% (v/v) ethanol (to 0.10% final concentrations in the organoid droplets). Induced-inhibited organoids were fed on day three with 1.36 μL feed droplets containing 14.6 mM ketoconazole and 0.146% (v/v) ethanol (to concentrations in the organoid droplet of 10.0 mM and 0.10%, respectively). For all conditions, one hour after the feeding on day three, 1.36 μL droplets of feed media containing 14.6 mM Vivid® BOMR dye (Life Technologies, Inc.) were added to each organoid culture to obtain a final dye concentration of 10.0 mM.

Two-dimensional macro-scale assays were performed for comparison. On day zero, 50 μL aliquots of PBS containing 0.1 mg mL^{-1} neutralized collagen I were dispensed into each well of tissue culture treated polystyrene flat-bottom 96 well plates (Corning, Inc.), incubated at 37 °C/5% CO_2 for 60 minutes, aspirated dry and allowed to air dry for 30 minutes in a laminar biosafety cabinet. 1.0×10^5 HepG2 cells and 3.0×10^4 NIH-3T3 cells were seeded into 100 μL feed medium per well and incubated at 37 °C/5% CO_2. Analogous three-day control, induced, and induced-inhibited conditions were defined and implemented as for DMF (as above). In place of GODEP, each feed was implemented by aspirating the well contents and replacing them with 100 μL aliquots of the new contents (to the same final concentrations as described above).

For both microscale and macroscale cultures, the fluorescence intensity was measured immediately upon adding the dye and every 15 minutes afterwards for 1 hour, with incubation at 37 °C/5% CO_2 between time-points, using a Pherastar multiwell plate reader (BMG Labtech) at 530/620 nm wavelength excitation/emission. Fluorescent intensity was normalized to the starting intensity for each culture droplet or culture well by baseline subtracting untreated controls. Enzymatic activity was estimated by the rate at which the fluorescent intensity increased over time.

Hepatotoxicity assay

Liver organoids were formed in the same manner as above except NIH-3T3s were excluded. After incubation at 37 °C/5% CO_2 for 24 h, a dilution series of droplets was formed on chip and merged with organoid cultures to final acetaminophen (acetyl-*para*-aminophenol or APAP) concentrations of 0, 5.0, 10.0 and 20.0 mM. Briefly, two 10.0 × 6.5 mm reservoirs were loaded with 12 μL of feed media containing either 2.93% (v/v) ethanol or 29.3 mM APAP and 2.93% ethanol. One 1.36 μL droplet of each concentration was dispensed, and the two droplets were merged and mixed by linear actuation across four 2.2 × 2.2 mm electrodes 5 times. The mixed droplet was split into two droplets of equal volume (each containing 14.7 mM APAP). A second 1.36 μL droplet of APAP-free feed media was dispensed and merged with one of the droplets containing 14.7 mM APAP, and subsequently mixed and split (as above) to form two droplets of equal volumes (each containing 7.3 mM APAP). One droplet containing 7.3 mM APAP was delivered to waste and then one additional 1.36 μL droplet was dispensed from each reservoir, leaving four 1.36 μL droplets of feed media containing 0, 7.3, 14.7 and 29.3 mM APAP. These droplets were then delivered to organoids using GODEP, forming final concentrations of 0, 5.0, 10.0 and 20.0 mM APAP. Organoids were then cultured for 24 hours at 37 °C/5% CO_2 before trinuclear staining by GODEP with 1.36 μL droplets of PBS containing 11.72 μM Hoescht 33342 (Life Technologies), 11.72 μM ethidium homodimer-1 and 7.33 μM NucView488 (Biotium, Inc., Hayward, CA, USA) with organoid culture droplets to obtain final concentrations of 8.00, 8.00 and 5.00 μM respectively. Excess media was removed and organoids were incubated at 37 °C/5% CO_2 for 60 minutes before washing with PBS droplets using GODEP and analyzed using a Nikon A1R confocal microscope system (Nikon Canada, Mississauga, Canada) by laser excitation at 408, 488 and 562 nm through a total of 22–23 *z*-dimension slices (spaced 10 μm apart) per organoid. For each condition conducted in duplicate, three predetermined photomicrographs of each organoid were selected for quantitation from (a) the center of the *z*-stack, (b) 40 μm above the center, and (c) 40 μm below the center. All photomicrographs were manually examined to ensure that no nuclei were counted multiple times. CellProfiler software (Broad Institute, Cambridge, MA, USA) was used to quantify the number of positive stained

cells on each channel using two class Otsu Global thresholding and weighted variance with a threshold correction factor of 0.7.

Results and discussion

Device design and operation

Microfluidic organoids for drug screening (MODS) is a new system that allows for the generation, culture and analysis of three dimensional liver-like microtissues. Each organoid is a free-floating 3D construct (~100–1000 μm diameter post-contraction) containing a hydrogel matrix and one or more types of cells (described in detail below). In contrast to all other microfluidic/liver techniques that we are aware of,[12–19] in MODS, each organoid is individually addressable, and thus can be used to probe the effects of an array of different conditions (*e.g.*, different INDs or different concentrations of IND) on individual trackable constructs over time. The MODS system relies on electrodynamic digital microfluidic (DMF) fluid manipulation, and a typical device is shown in Fig. 1A.

In developing MODS, we determined that a key requirement was the ability to work with free-floating microtissues to allow for cell-driven contraction and remodeling. This presents a challenge for fluid exchange – in all previous DMF methods for working with mammalian cells, fluids were exchanged for cells adhered to a device surface[22–24] or embedded in an adhered matrix.[27,28] To accommodate fluid exchange for free-floating microtissues, the MODS system was designed to include arrays of microposts that serve as retention barriers to confine organoids to predetermined locations. Rectangular and oval microposts were evaluated and were found to be equally effective at organoid confinement (data not shown). However, oval microposts more consistently permitted droplets to merge across the posts (Fig. 1D "step 3") (data not shown) and were subsequently used for most experiments. The only previous report of this type of physical barrier in a DMF system that we are aware of was reported by Mousa *et al.*,[35] who used the barriers for an unrelated purpose (to aid in partitioning non-mixing solvents for liquid–liquid extraction).

In initial experiments, a general organoid droplet exchange procedure (GODEP) was developed (Fig. 1D), which is described in detail in the experimental section. Briefly, one or more droplets of feed media or other reagents are driven to organoid culture regions and subsequently merged and mixed with the organoid-containing droplets. Excess media is then driven to a waste reservoir or is saved for subsequent analysis. Reagent concentrations are thus diluted to known concentrations, and multiple GODEPs can be implemented sequentially to further concentrate or dilute reagents when required. A detailed examination of droplet mixing during GODEP is described in the online ESI.† In typical experiments, organoids were cultured on-chip for several days using GODEP to exchange culture media every 24 hours.

Organoid characterization

The 3D organoids described here were designed to recapitulate *in vivo* liver function more accurately than conventional 2D *in vitro* cell culture. In practice, HepG2 cells were embedded in 3D hydrogel matrices comprising collagen I, a native extracellular matrix protein known to direct cells into phenotypes that more closely resemble those found *in vivo*.[36] In addition, we evaluated the use of NIH-3T3 fibroblasts as a component of the DMF liver organoids, as they are known to actively remodel hydrogels[10] and provide biochemical signals required for liver cell activity.[37]

Three metrics were used to characterize liver organoids: construct contractility, viability and albumin production. For the first metric, cells grown in hydrogel matrices are known to remodel and contract their local microenvironments. This effect is an important parameter to measure for a number of reasons. First, even a modest hydrogel contraction can significantly increase cell densities. For example, an isometric contraction to half the original length scales results in an 8-fold reduction in total volume, or an 8-fold increase in cell density (before accounting for cell division or other processes). This allows for the study of cell densities that are close to those of native tissue (~10^9 cell cm^{-3} in liver[38]). Second, hydrogel contraction coupled with matrix protein remodeling can increase the likelihood of cells coming into physical contact with each other, which may be important because hepatocyte–hepatocyte contact is known to inhibit division-related processes while increasing liver-specific functions.[39] Third, hydrogel contraction also increases matrix stiffness, which affects a wide range of cellular processes including growth, morphology and migration.[40]

Fig. 2A depicts representative liver organoids evaluated in contractility assays. HepG2 cells were seeded with or without 2×10^6 cell mL^{-1} NIH-3T3 cells and at 'low' (0.9 mg mL^{-1}) or 'high' (1.5 mg mL^{-1}) collagen I concentrations and were evaluated on day zero and after four days in culture. As expected, the presence of NIH-3T3 fibroblasts substantially increased the contraction over 4 days relative to organoids without fibroblasts. Collagen density also played a role in this process, with high collagen density slightly inhibiting the magnitude of contraction. The presence or absence of fibroblasts at the concentrations used in this study had a greater impact on the contraction than did the change in collagen density. Importantly, the diameter of organoids, even when seeded with NIH-3T3 cells in low density collagen, did not decrease to smaller than the gaps in the retention barrier (~50 μm). Similar levels of contraction in microgels seeded with fibroblasts have been reported previously for pooled systems[10] (*i.e.*, many microgels in a chamber). However, as far as we are aware this is the first report of work in which the contraction of individually addressable hydrogel constructs can be monitored over time. We propose that MODS is uniquely well suited for creating individually suspended hydrogels on an open platform which are free to contract in three dimensions.

For the second characterization metric for liver organoids, viabilities were assessed to determine the effects of culture conditions, including the degree of contraction, on cell health. As shown in Fig. 2B, the majority of cells remained viable after four days in culture as determined by calcein-AM

staining, with few dead cells (determined by ethidium homodimer-1 staining) observed in any of the tested conditions. This suggests that there is adequate diffusion of nutrients into and adequate diffusion of waste products out of hydrogel organoids. Contraction and viability measures together provided an approximate measure of cell health and activity.

For the third characterization metric for liver organoids, albumin production was chosen as a general measure of liver functional activity.[41] To assay the amount of albumin secreted, media was collected during daily feeds from MODS cultures using GODEP (Fig. 1D) and assayed for human albumin. As shown in Fig. 3, for the first 3 days, no significant difference in albumin levels was observed between HepG2 organoids and HepG2/NIH-3T3 organoids, but by day 4, the co-cultured organoids generated significantly ($p < 0.05$) greater levels of albumin ($1.03 \times 10^4 \pm 1.40 \times 10^3$ ng mL^{-1}) than mono-culture organoids ($3.24 \times 10^3 \pm 1.39 \times 10^3$ ng mL^{-1}). This finding is consistent with previous results,[11,42,43] confirming that co-culture with fibroblasts improves the functional activity of HepG2 hepatocytes and may be related to the contractility of the organoids as described above. Interestingly, there were no statistical differences in albumin levels between organoids cultured in low or high collagen densities.

The results described above confirm that the MODS technique can be used to form and maintain viable 3D liver organoids with robust hepatocyte activity on-chip for multiple days. To evaluate the suitability of MODS for drug screening, two common assays were evaluated: CYP activity and hepatotoxicity. Fully contracted organoids formed with low concentration of collagen (0.9 mg mL^{-1}) were used in these experiments, which are described below.

CYP enzymatic activity

Cytochrome P450 (CYP) is a superfamily of proteins found primarily in the liver which are responsible for the catalysis of organic substances.[44] These enzymes are of particular interest to the pharmaceutical industry because they metabolize many drugs and antibiotics. In addition, some small molecules are known to interfere with CYP enzymatic activity, delaying the clearance of other drugs or toxins *in vivo*.[45] In this work, we evaluated the activity of human Cytochrome P450 isoform 3A4 (CYP3A4) in liver organoids after incubation with compounds known to either induce or inhibit CYP3A4 enzymatic activity. Dexamethasone, an anti-inflammatory and immunosuppressant drug was used as a model CYP3A4 inducer, and ketoconazole, an anti-fungal drug, was used as a model CYP3A4 inhibitor. CYP3A4 activity was monitored using a fluorogenic substrate (BOMR) with specificity to CYP3A4[46,47] in no treatment, induced, or induced-inhibited HepG2/NIH-3T3 co-cultures. The cultures were grown either as 2D monolayers in well plates or as 3D organoids in DMF devices. As shown in Fig. 4A, the rates of substrate metabolism (as determined by the slopes of the curves) by HepG2/NIH-3T3 co-cultured cells in 2D monolayers in well-plates were indistinguishable, regardless of the

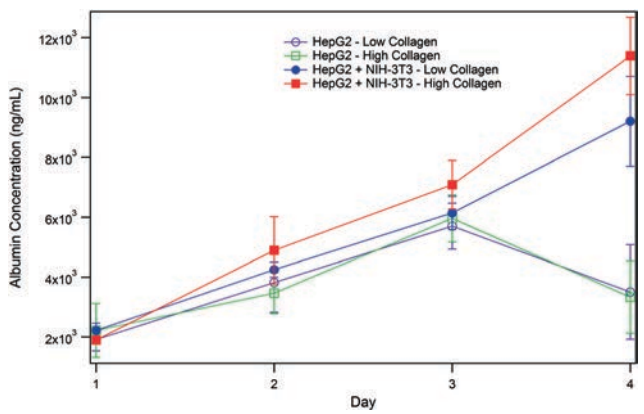

Fig. 3 Organoid albumin secretion assay. Concentration of secreted albumin in liver organoid media collected during daily feeds determined using an ELISA for human albumin. Organoids were created with HepG2 cells, with (closed symbols) or without (open symbols) NIH-3T3 fibroblasts and in either low (0.9 mg mL^{-1}) (purple/blue circles) or high (2.9 mg mL^{-1}) (red/green squares) collagen. Error bars represent ±1 standard deviation, n = 3.

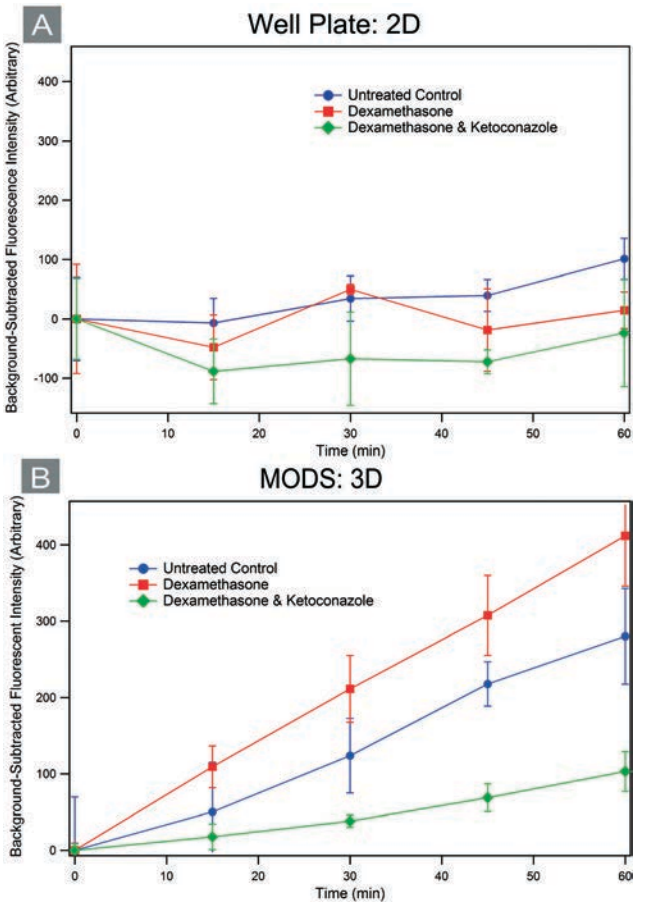

Fig. 4 Organoid cytochrome P450 3A4 assay. HepG2 and NIH-3T3 laden organoids were untreated (blue circles), incubated with 10 mM dexamethasone for 48 hours prior to assay (red squares), or incubated with 10 mM dexamethasone for 48 hours plus 10 mM ketoconazole for 1 hour (green diamonds) prior to assay. Assays and cultures were conducted on HepG2/NIH-3T3 co-cultures in (A) two-dimensional format in 96 well plates or (B) three-dimensional organoids by MODS. Error bars represent ±1 standard deviation, n = 3.

treatment condition. In contrast, the rates of substrate metabolism were clearly distinguishable in 3D DMF-cultured organoids (Fig. 4B). Dexamethasone-treated organoids demonstrated a significantly higher rate ($p < 0.05$) of BOMR metabolism (slope of 6.86 ± 0.77 intensity units min^{-1}) and ketoconazole-treated organoids significantly lower ($p < 0.01$) metabolism (slope of 1.72 ± 0.57 intensity units min^{-1}) than untreated control organoids (slope of 4.67 ± 0.20 intensity units min^{-1}). The differences in slopes were consistent with the expected changes to CYP activity as a result of treatment with chemical inducers and inhibitors. Hepatocyte CYP activity has been shown to be higher in three dimensional systems than in traditional two dimensional formats,[48] which may explain the higher HepG2 liver-specific function in the DMF platform relative to conventional 2D cultures. Another attribute of the DMF system which may contribute to this difference may be that the detection limits for fluorescent read-outs on DMF devices are often superior to those of comparable assays implemented on macroscale well plates,[33] a phenomenon that is likely a result of increased signal from the reflective metal layer on devices.

It should be noted that the HepG2 cells used here (an inexpensive immortalized cell line) are typically not used in metabolism tests because of the inability of 2D HepG2 cell cultures to model CYP activity.[49,50] For example, Gerets *et al.*[49] reported no significant differences in transcriptional regulation for human CYP3A4 in HepG2 cells in response to treatment with known CYP inducers, beta-naphtoflavone, phenobarbitol and rifampicin. This is consistent with the data in Fig. 4A, which reveals 2D HepG2 culture to be a poor model for evaluating the effects of dexamethasone and ketoconazole on CYP activity. But as shown in Fig. 4B, the CYP activity of DMF-cultured organoids containing HepG2 immortalized cells can be both induced and repressed by small molecules. Also, in contrast to assays that use RNA quantification as an indirect measure of enzyme activity (*i.e.*, qPCR for CYP), the MODS platform allows direct quantification of the relative rates of the CYP activities in real time. If similar responses can be observed for other compounds, this will be a particularly attractive feature of the DMF organoid model system for screening CYP activity in inexpensive immortalized cells without resorting to expensive primary hepatocytes.

Hepatoxicity

For a "fail early, fail cheaply"[2] paradigm of drug development to succeed, IND candidates with the potential for adverse human effects must be identified through routine screens. To evaluate the MODS platform for hepatoxicity screening, acetaminophen (APAP)-induced hepatotoxicity was chosen for a proof of principle study since APAP overdose accounts for 39% of acute liver failure cases in the United States.[5] The MODS system is particularly well suited for this application because of its ability to replace labour intensive processes with automated on-chip droplet manipulation. Fig. 5A depicts the on-chip formation of a 4 point serial dilution curve used to evaluate the cytotoxicity of a range of APAP concentrations on individual organoids. In the future, this function might be combined with on-chip electrochemical quantitation of APAP[51] to achieve finer control over concentrations, but the four-point system used here was useful to evaluate the concept.

HepG2-laden organoids were formed and then exposed to 0, 5.0, 10.0 or 20.0 mM APAP for 24 h using the MODS platform. Confocal photomicrograph stacks of APAP-treated organoids from this study are shown in Fig. 5B. The percentage of cells positively stained for early apoptosis (by caspase-3) and necrosis (by ethidium homodimer-1) were determined from these photomicrographs (Fig. 5C). As shown, APAP

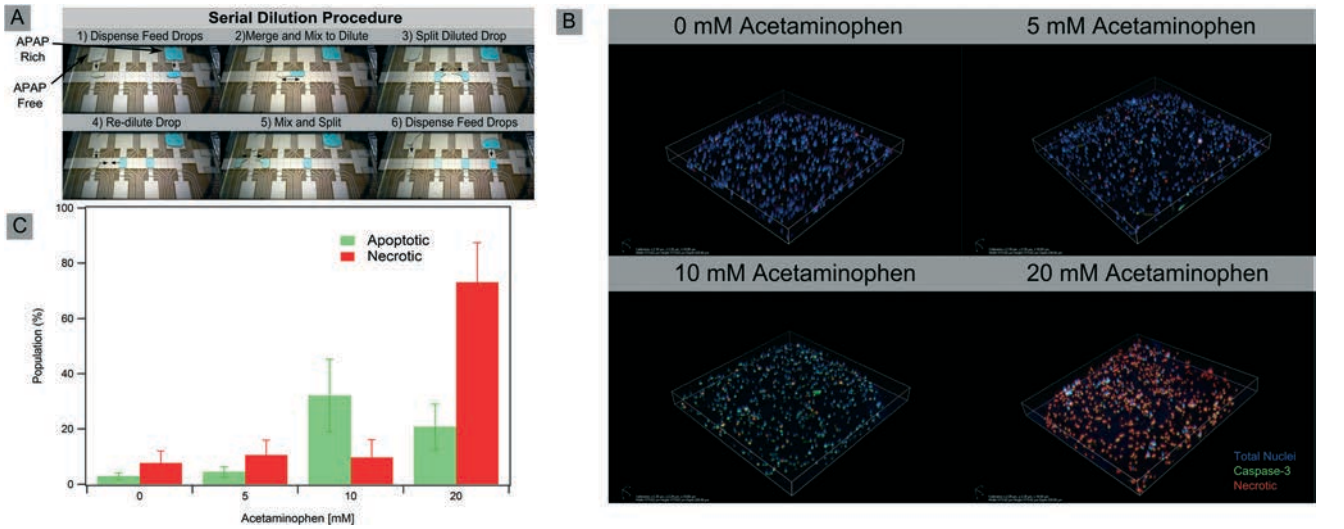

Fig. 5 Organoid acetaminophen (APAP) hepatotoxicity assay. (A) Images from a movie illustrating a serial dilution procedure for generating 0, 5.0, 10.0 or 20.0 mM acetaminophen. (B) Confocal stacks of organoids trinuclear stained for total nuclei (blue), caspase-3 (green) and necrotic cells (red). (C) Percentage of apoptotic (shaded green bars) and necrotic (solid red bars) cells in organoids analyzed by CellProfiler software in three predetermined slices per organoid. Error bars represent ±1 standard deviation, $n = 2$.

treatment at 5.0 mM did not result in apoptotic (green bars) or necrotic (red bars) responses relative to control cultures. This contrasts with treatment with 10.0 mM APAP, which are consistent with increased levels of apoptosis (32.0 ± 13.2% for caspase-3) while treatment at 20.0 mM APAP suggests that there may be increased apoptosis (20.7 ± 8.2% for caspase-3) and necrosis (73.2 ± 14.2% for ethidium homodimer-1) relative to untreated controls. Further studies are needed to validate this proof of principle work, but the observed shift from predominately programmed death at 10.0 mM APAP to necrotic-dominated death at 20.0 mM is consistent with dose and time-dependent responses of hepatoma cells treated with APAP and other drugs *in vitro*.[52,53]

The data described above was generated on an automated platform that carries out on-chip IND dilution, long-term 3D organoid culture, and on-chip toxicity assays. In the future, we propose to generate larger devices capable of evaluating several drugs in parallel (perhaps using new techniques to form DMF devices with thousands of individually addressable electrodes[54]); if successful, we propose that such systems may be a useful new tool for high throughput drug development.

Conclusions

Here, we have introduced the *microfluidic organoids for drug screening* (MODS) platform, which is capable of generating arrays of individually addressable, free-floating hydrogel-based microtissues. In this proof of principle work, we focused on a hepatic tissue model, and applied the system to two assays that are commonly used in the pharmaceutical industry: CYP enzymatic activity and hepatotoxicity. In the future, we propose that the MODS system can be expanded to conduct a larger number of additional assays, such as the panel of preclinical assays mandated by the FDA. Likewise, other organ systems may be compatible with this system, formed by incorporating different cell types and various other hydrogels. Thus, we propose that MODS is a promising development in the goal of developing "fail early, fail cheaply" strategies for drug screening.

Acknowledgements

We thank the Natural Sciences and Engineering Research Council of Canada (NSERC), the Canadian Institutes of Health Research (CIHR), the Ontario Research Excellence Fund, and the Ontario Institute for Cancer Research (OICR) for financial support. S.H.A. thanks NSERC for a graduate fellowship, M.D.C thanks CHIR for a post-doctoral fellowship and A.R.W. thanks the Canada Research Chair (CRC) Program for a CRC. We thank Dr. Korkut Uygun (Harvard Medical School) for constructive conversations.

References

1 S. M. Paul, D. S. Mytelka, C. T. Dunwiddie, C. C. Persinger, B. H. Munos, S. R. Lindborg and A. L. Schacht, *Nat. Rev. Drug Discovery*, 2009, **9**, 203–214.
2 L. Safinia, in *Frost & Sullivan Market Reports*, 2008.
3 US Food and Drug Administration, *Innovation or stagnation: challenge and opportunity on the critical path to new medical products*, 2004, http://www.fda.gov/ScienceResearch/SpecialTopics/CriticalPathInitiative/CriticalPathOpportunitiesReports/ucm077262.htm.
4 J. P. Hughes, S. Rees, S. B. Kalindjian and K. L. Philpott, *Br. J. Pharmacol.*, 2011, **162**, 1239–1249.
5 G. Ostapowicz, R. J. Fontana, F. V. Schiodt, A. Larson, T. J. Davern, S. H. B. Han, T. M. McCashland, A. O. Shakil, J. E. Hay, L. Hynan, J. S. Crippin, A. T. Blei, G. Samuel, J. Reisch, W. M. Lee and U. S. A. L. F. S. Grp, *Ann. Intern. Med.*, 2002, **137**, 947–954.
6 Y. S. Torisawa, A. Takagi, Y. Nashimoto, T. Yasukawa, H. Shiku and T. Matsue, *Biomaterials*, 2007, **28**, 559–566.
7 F. J. Wu, J. R. Friend, C. C. Hsiao, M. J. Zilliox, W. J. Ko, F. B. Cerra and W. S. Hu, *Biotechnol. Bioeng.*, 1996, **50**, 404–415.
8 T. T. Chang and M. Hughes-Fulford, *Tissue Eng., Part A*, 2009, **15**, 559–567.
9 C. M. Hwang, S. Sant, M. Masaeli, N. N. Kachouie, B. Zamanian, S.-H. Lee and A. Khademhosseini, *Biofabrication*, 2010, **2**, 035003.
10 A. P. McGuigan, D. A. Bruzewicz, A. Glavan, M. Butte and G. M. Whitesides, *PLoS One*, 2008, **3**, 11.
11 S. J. Seo, I. Y. Kim, Y. J. Choi, T. Akaike and C. S. Cho, *Biomaterials*, 2006, **27**, 1487–1495.
12 Y.-C. Toh, T. C. Lim, D. Tai, G. Xiao, D. van Noort and H. Yu, *Lab Chip*, 2009, **9**, 2026–2035.
13 C. Zhang, Z. Q. Zhao, N. A. A. Rahim, D. van Noort and H. Yu, *Lab Chip*, 2009, **9**, 3185–3192.
14 V. N. Goral, Y. C. Hsieh, O. N. Petzold, J. S. Clark, P. K. Yuen and R. A. Faris, *Lab Chip*, 2010, **10**, 3380–3386.
15 L. Ma, J. Barker, C. C. Zhou, W. Li, J. Zhang, B. Y. Lin, G. Foltz, J. Kublbeck and P. Honkakoski, *Biomaterials*, 2012, **33**, 4353–4361.
16 K. H. Lee, S. J. Shin, C. B. Kim, J. K. Kim, Y. W. Cho, B. G. Chung and S. H. Lee, *Lab Chip*, 2010, **10**, 1328–1334.
17 K. Viravaidya, A. Sin and M. L. Shuler, *Biotechnol. Prog.*, 2004, **20**, 316–323.
18 B. J. Kane, M. J. Zinner, M. L. Yarmush and M. Toner, *Anal. Chem.*, 2006, **78**, 4291–4298.
19 J. E. Snyder, Q. Hamid, C. Wang, R. Chang, K. Emami, H. Wu and W. Sun, *Biofabrication*, 2011, **3**, 9.
20 F. Mugele and J. C. Baret, *J. Phys.: Condens. Matter*, 2005, **17**, R705–R774.
21 A. R. Wheeler, *Science*, 2008, **322**, 539–540.
22 I. Barbulovic-Nad, S. H. Au and A. R. Wheeler, *Lab Chip*, 2010, **10**, 1536–1542.
23 D. Bogojevic, M. D. Chamberlain, I. Barbulovic-Nad and A. R. Wheeler, *Lab Chip*, 2012, **12**, 627–634.
24 S. C. C. Shih, I. Barbulovic-Nad, X. Yang, R. Fobel and A. R. Wheeler, *Biosens. Bioelectron.*, 2013, **42**, 314–320.
25 S. K. Fan, P. W. Huang, T. T. Wang and Y. H. Peng, *Lab Chip*, 2008, **8**, 1325–1331.
26 S. H. Au, S. C. C. Shih and A. R. Wheeler, *Biomed. Microdevices*, 2011, **13**, 41–50.

27 L. K. Fiddes, V. N. Luk, S. H. Au, A. H. C. Ng, V. Luk, E. Kumacheva and A. R. Wheeler, *Biomicrofluidics*, 2012, 6.
28 I. A. Eydelnant, B. B. Li and A. R. Wheeler, *Nat. Commun.*, 2014, **5**, 3355.
29 S. Srigunapalan, I. A. Eydelnant, C. A. Simmons and A. R. Wheeler, *Lab Chip*, 2012, **12**, 369–375.
30 S. H. Au, R. Fobel, S. P. Desai, J. Voldman and A. R. Wheeler, *Integr. Biol.*, 2013, **5**, 1014–1025.
31 R. Fobel, A. E. Kirby, A. H. C. Ng, R. R. Farnood and A. R. Wheeler, *Adv. Mater.*, 2014, **26**, 2838–2843.
32 S. H. Au, P. Kumar and A. R. Wheeler, *Langmuir*, 2011, **27**, 8586–8594.
33 I. Barbulovic-Nad, H. Yang, P. S. Park and A. R. Wheeler, *Lab Chip*, 2008, **8**, 519–526.
34 R. Fobel, C. Fobel and A. R. Wheeler, *Appl. Phys. Lett.*, 2013, **102**, 193513–193515.
35 N. A. Mousa, M. J. Jebrail, H. Yang, M. Abdegawad, P. Metalnikov, J. Chen, A. R. Wheeler and R. F. Casper, *Sci. Transl. Med.*, 2009, **1**, 1ra2.
36 M. W. Tibbitt and K. S. Anseth, *Biotechnol. Bioeng.*, 2009, **103**, 655–663.
37 V. L. Tsang, A. A. Chen, L. M. Cho, K. D. Jadin, R. L. Sah, S. DeLong, J. L. West and S. N. Bhatia, *FASEB J.*, 2007, **21**, 790–801.
38 A. P. McGuigan and M. V. Sefton, *Proc. Natl. Acad. Sci. U. S. A.*, 2006, **103**, 11461–11466.
39 T. Nakamura, K. Yoshimoto, Y. Nakayama, Y. Tomita and A. Ichihara, *Proc. Natl. Acad. Sci. U. S. A.*, 1983, **80**, 7229–7233.
40 R. G. Wells, *Hepatology*, 2008, **47**, 1394–1400.
41 A. Farrugia, *Transfus. Med. Rev.*, 2010, **24**, 53–63.
42 E. E. Hui and S. N. Bhatia, *Proc. Natl. Acad. Sci. U. S. A.*, 2007, **104**, 5722–5726.
43 A. Ito, H. Jitsunobu, Y. Kawabe and M. Karnihira, *J. Biosci. Bioeng.*, 2007, **104**, 371–378.
44 S. A. Wrighton and J. C. Stevens, *Crit. Rev. Toxicol.*, 1992, **22**, 1–21.
45 J. H. Lin and A. Y. H. Lu, *Clin. Pharmacokinet.*, 1998, **35**, 361–390.
46 N. J. Liptrott, M. Penny, P. G. Bray, J. Sathish, S. H. Khoo, D. J. Back and A. Owen, *Br. J. Pharmacol.*, 2009, **156**, 497–508.
47 O. Trubetskoy, B. Marks, T. Zielinski, M. F. Yueh and J. Raucy, *AAPS J.*, 2005, **7**, E6–E13.
48 K. Nakamura, R. Mizutani, A. Sanbe, S. Enosawa, M. Kasahara, A. Nakagawa, Y. Ejiri, N. Murayama, Y. Miyamoto, T. Torii, S. Kusakawa, J. Yamauchi, M. Fukuda, H. Yamazaki and A. Tanoue, *J. Biosci. Bioeng.*, 2011, **111**, 78–84.
49 H. H. Gerets, K. Tilmant, B. Gerin, H. Chanteux, B. O. Depelchin, S. Dhalluin and F. A. Atienzar, *Cell Biol. Toxicol.*, 2012, **28**, 69–87.
50 P. M. van Midwoud, E. Verpoorte and G. M. M. Groothuis, *Integr. Biol.*, 2011, **3**, 509–521.
51 M. D. M. Dryden, D. D. G. Rackus, M. H. Shamsi and A. R. Wheeler, *Anal. Chem.*, 2013, **85**, 8809–8816.
52 I. Manov, M. Hirsh and T. C. Iancu, *Exp. Toxicol. Pathol.*, 2002, **53**, 489–500.
53 I. Manov, M. Hirsh and T. C. Iancu, *Pharmacol. Toxicol.*, 2004, **94**, 213–225.
54 B. Hadwen, G. R. Broder, D. Morganti, A. Jacobs, C. Brown, J. R. Hector, Y. Kubota and H. Morgan, *Lab Chip*, 2012, **12**, 3305–3313.